

MEASUREMENTS OF ELECTRON COOLING RATES
IN THE MIDLATITUDE AND
AURORAL ZONE THERMOSPHERE

L. H. Brace, H. G. Mayr
and G. R. Carignan

ABSTRACT

Two day-night pairs of Thermosphere Probe rockets, launched at Wallops Island, Virginia in March of 1965 and at Churchill, Manitoba in November of 1965, have provided altitude profiles of electron temperature and concentration at mid-day and midnight. Altitude profiles of N_2 measured on the same four flights have in addition provided neutral gas temperature profiles. These data are employed to calculate electron cooling rate profiles, and these in turn are interpreted in terms of ionospheric heat sources. The daytime electron heat source for the F-region, at both middle latitudes ($L = 2.9$) and in the auroral zone ($L \approx 8$), appears consistent with solar ultraviolet heating. The nighttime F-region however appears to be heated by downward conduction from the protonosphere at middle latitudes and by particle heating in the auroral zone.

The source of electron heating for the E-region both day and night and at both locations cannot be explained by direct solar heating. This may be produced by neutral winds, electric currents, an unknown chemical reaction or, as Walker has suggested, selective heating of the electrons by excited N_2 having lifetimes in the E-region of the order of a day.

INTRODUCTION

The sources of heat for the upper atmosphere have been a matter of interest for many years. In the past few years it has been apparent that the electron temperature (T_e) in the ionosphere is a very sensitive indicator of this heating (Hanson, 1963) (Dalgarno, McElroy and Moffett, 1963). Much of the thermal energy of the upper atmosphere originates as excess energy of the photoelectrons produced by photoionization, and much of this excess energy is shared with the ambient thermal electrons thereby raising their temperature above that of the ions and neutrals.

In the lower F-region and E-region the thermal electrons cool locally to the ions and the neutrals through both elastic and inelastic collisions. In the F-region and above the electrons are heated by escaping fast electrons and are either heated or cooled by thermal conduction within the electron gas.

Considerable progress has been made recently toward understanding the electron heat balance. Dalgarno, McElroy and Walker (1967), starting with a measured solar euv flux and models of the neutral atmosphere, were able to calculate electron temperature profiles which are in good agreement with those measured on rocket flights (Brace, Spencer, Carignan, 1963) (Spencer, et al., 1965). Some difficulty was encountered in reproducing the measured F_1 -region temperatures, the calculated values being too high. This may now have been explained by the introduction of a new cooling mechanism associated with excitation of the fine structure levels of atomic oxygen (Dalgarno and Degges, 1967) (Dalgarno, et al., 1968).

Upper F-region daytime temperatures measured by rockets and satellites appear also to be explained in terms of non-local heating by escaping fast electrons (Brace, Spencer, and Dalgarno, 1965) and by thermal conduction downward from the protonosphere (Brace and Reddy, 1965) (Dalgarno, et al., 1967) (Nagy and Walker, 1967).

The electron temperature in the E-region has been found by various probe techniques to be significantly higher than the gas temperature, a result which is not consistent with E-region temperatures inferred from radar backscatter observations and is not easily understood in terms of solar ultraviolet heating (Spencer, et al., 1965). On the other hand Walker (1967) has related the elevated E-region temperatures to high vibrational temperatures of molecular nitrogen.

One objective of the two day-night pairs of launchings reported here was to further investigate the energy balance of the thermosphere, with particular emphasis on the differences between the heat sources at the two locations of Wallops Island ($L = 2.9$) and Churchill ($L = 8$).

THE ELECTROSTATIC PROBE EXPERIMENT

The cylindrical probe employed on the Thermosphere Probe payloads has been described by Spencer, et al., (1965). In principle, a thin cylindrical collector is immersed in the plasma surrounding the instrument, and the volt-ampere characteristic of the sensor is recorded. The amplitude of the electron current waveform is directly proportional to the electron concentration (N_e) and the

curvature of the electron retarding region relates directly to the electron temperature (T_e).

The electrical arrangement of the experiment is shown schematically in Figure 1. The collector is 23 cm in length, 0.06 cm in diameter, and is isolated from the body of the instrument by a guard electrode which is 15 cm long. Both elements of the sensor are made of stainless steel. The entire sensor is spring-loaded so that it lies within the clam-shell nose cone and is self-erecting when ejection of the instrument takes place, typically at 80 kilometers altitude.

A sawtooth voltage, V_a , is applied to both the collector and guard electrode, while only the collector current is measured and telemetered to earth. The repetition rate of the sweep is about 6 per second, and two amplitudes are employed alternately (-3 to +5v, -1 to +1.75v). The current waveforms are resolved by three current ranges having full scale sensitivities of 0.1 μa , 1 μa , and 10 μa on the night flights and 0.3 μa , 3 μa and 30 μa respectively on the day flights.

The radius of the collector assures that the current collection is orbit-motion-limited (Mott-Smith, and Langmuir, 1926) over the entire range of N_e encountered in flight. The collector is long enough to make the electrical end effects at the outer end negligible. This has been verified on one of these flights (NASA 18.02), as well as on two previous flights, by removing the normal sweep voltage from the guard electrode occasionally and alternately grounding it to the housing or allowing it to float at its own rest potential. In both cases, a negligible increase in electron current is observed (<5%) in the electron saturation region. No other effects of the undriven guard were noted.

In flight, the instrument is ejected at about 80 kilometers from its clam shell nose cone which is designed to impart a tumbling motion to the entire instrument. A three second tumble period is nominal. The instrument tumbles upward through the thermosphere to a peak altitude of about 330 kilometers, separating from the vehicle at a rate of about one meter per second. During the entire nine-minute flight approximately 3000 volt-ampere characteristics are recorded, about half of these in the proper current range for determining either T_e or N_e . Both the upleg and downleg portions of the flight provide valid data, with the possible reservation that the early upleg data may occasionally exhibit some rocket contamination effects until a large enough separation from the vehicle has been achieved.

THE OBSERVATIONS

Table I lists the information concerning the four flights to be discussed. The $F_{10.7}$ refers to the 10.7 cm index of solar activity, and a_p is the 3-hour planetary magnetic index. All flights were made on magnetically quiet days at solar minimum. The pair of Wallops launches corresponded to spring equinox and the Churchill pair, although planned originally for fall equinox, were launched about midway between the fall equinox and winter solstice. The T_e and N_e measurements from these flights are given in Table II and are shown in Figures 2 through 9. The corresponding N_e profiles derived from simultaneously recorded ionograms are also shown (courtesy J. W. Wright). Although the agreement between the probe and ionosonde N_e values is better than 20% at the

F_2 maximum on all flights, the agreement at lower altitudes varies markedly. A downward shift of the 6.11 ionosonde data (Figure 2) by 10 kilometers would greatly improve the agreement between 200 and 250 kilometers, but the probe data would remain 15% high at the F_2 maximum. A similar downward shift of the 18.01 ionosonde profile would better fit the lower boundary of the E-region as defined by the probe data.

In the 18.02 ionosonde data, the entire F-region appears to be displaced downward from the rocket data by about 30 kilometers, although the E-region data agree very well in magnitude and shape. Such comparisons in this flight should be viewed with particular caution however, since Walker, Brace and Rees (1968) have shown that particle precipitation was probably responsible for creating and heating this nighttime ionosphere. Thus the usual reservations about temporal and spatial gradients are even more valid in this comparison.

The E-region of NASA 18.03 provides the greatest disagreement yet observed between the probe and ionosonde measurements. Although the agreement is good near 180 kilometers, the probe values are consistently high from 90 kilometers to 170 kilometers. The difference approaches a factor of two in the E-region. The upleg-downleg agreement suggests that horizontal and temporal variations are not likely to be responsible for the probe-ionosonde disagreement.

If the probe measurements of N_e in the E-region are indeed sometimes enhanced it appears that too few data are available from this series to identify the cause. The single nighttime flight which has ionosonde data for comparison

exhibits good agreement (NASA 18.02), while the daytime flight 11 hours earlier at the same site shows the greatest disagreement (18.03). From this, one might conclude that the enhanced current collection is somehow related to the effects of solar radiation on the atmosphere or on the instrument. Neither of these is easy to explain.

Photoelectrons emitted from the stainless steel surface of the instrument housing could not produce a current at the collector which would compete with the random electron current from the plasma (order of 10^{-6} amperes cm^{-2}). Measurements of the photo electron current leaving the stainless steel collector itself place an upper limit at about 10^{-8} amperes cm^{-2} . It is difficult to imagine a collection scheme which would enhance the current reaching the probe by two orders of magnitude, since the full accelerating voltage enhances the thermal electron current by only a factor of about four over the random electron current.

DISCUSSION

To permit comparison of these four flights in terms of ionospheric heat sources, we have calculated the rates of electron cooling, L_e , for the downleg of each flight. Since the cooling rate depends in part upon the ion temperature, we first calculate the ion temperature by equating the rate at which ions are heated by the electrons

$$L_{ei} = \frac{5 \times 10^{-7} (T_e - T_i) N_e n(O^+)}{T_e^{3/2}} \quad (2)$$

to the rate at which the ions cool to the neutrals (Brace, et al., 1965) (Dalgarno and Walker, 1967),

$$L_{in} = n(O^+) \left\{ 1.8 \times 10^{-13} n(O) + 6 \times 10^{-14} n(N_2) + 6 \times 10^{-15} n(H_e) + 2 \times 10^{-15} n(H) \right\} (T_i - T_g) \quad (3)$$

We consider only the energy loss processes involving O^+ because the light ion concentrations are negligible at the altitude of these flights and molecular ions are neglected since they become dominant only at lower altitudes where the difference between ion and neutral temperature is negligible. The explicit expression for T_i given by Dalgarno, et al., (1967) is

$$T_i = T_g + \frac{5 \times 10^{-7} (T_e - T_g)}{T_e^{3/2}} N_e^2 \left\{ \frac{5 \times 10^{-7} N_e^2}{T_e^{3/2}} + N_e \left[1.8 \times 10^{-13} n(O) + 6 \times 10^{-14} n(N_2) + 6 \times 10^{-15} n(H_e) \right] \right\}^{-1} \quad (4)$$

Figures 10 through 13 show the calculated values of T_i , the measured values of T_e , N_e and the model value of T_g employed.

Since the electrons cool to both the ions (L_{ei}) and the neutrals (L_{en}), both loss rates must be considered, i.e.,

$$L_e = L_{ei} + L_{en} \quad (5)$$

The loss rate to the neutrals is given by

$$L_{en} = 1.34 \times 10^{-4} N_e \left[A n(N_2) + B n(O_2) + C n(O) + D n(H_e) \right] \quad (6)$$

where the coefficient A is according to Dalgarno, McElroy, Rees and Walker, (1968), and the coefficients B and D are due to Banks, (1966). Coefficient C contains the elastic collision term according to Banks (1966) and inelastic terms due to Dalgarno, et al., (1968), Dalgarno and Degges (1967), and Rees, Walker and Dalgarno (1967).

The gas temperatures employed in the calculations were derived from a Jacchia Model (Jacchia, 1965) which was selected in each case to have an exospheric temperature in agreement with that derived from the N₂ scale height measured on that particular flight (Spencer, et al., 1967). The neutral particle concentrations were also taken from the corresponding model. The resulting electron cooling rates for these flights are shown in Figure 14. An ev heating rate calculated by Dalgarno, et al., (1967) for similar daytime conditions is also shown.

INTERPRETATION

The seven month interval between the Wallops launchings (March 1965) and the Churchill launchings (November 1965) requires that any inferences regarding latitudinal variation be viewed with appropriate caution. On the other hand, the diurnal variation at each location should be resolved accurately as the rockets were launched in day-night pairs only 12 hours apart.

Daytime—The daytime electron loss rates at Wallops and Churchill are in excellent agreement, and both agree well above 160 kilometers with the ev heating rate calculated by Dalgarno, et al., (1967). The cooling rates below 160

kilometers diverge from that predicted from euv, and this will be discussed later. From the F-region agreement, however, it appears that euv remains the primary source of heating for the daytime auroral zone F-region. The slightly lower values of L_e at Churchill near 200 kilometers may reflect the higher solar zenith angle of 77° at Churchill as compared with 41° at Wallops.

The role of electron heat conduction is essentially negligible in the electron heat balance at all altitudes in two daytime flights 18.01 and 18.03. The positive temperature gradients at both Wallops Island and Churchill reflects a downward conduction of heat. The corresponding heating rate at 300 kilometers is about an order of magnitude less than the local heating and cooling rates at both locations.

The nighttime—From the good daytime agreement between the Wallops and Churchill L_e profiles it follows that the nighttime profiles may accurately reflect real latitudinal differences in the nocturnal heat sources. The nighttime L_e profiles appear to reflect quite different sources of heating at these two locations. Walker, et al., (1968) have analyzed the Churchill profile and concluded that the heating between 150 and 250 kilometers and the E-region ionization can be explained by electron precipitation. The fact that (1) these fluxes could be present continuously without producing a visible aurora and (2) the existence of this kind of nocturnal E-region is normal at Churchill, suggests that the results of this flight may be typical.

The nocturnal heating at Wallops is much smaller than observed at Churchill, except above 300 kilometers. The Wallops profile exhibits a generally irregular structure but shows a tendency to increase with altitude between 200 kilometers and apogee. One should not place much confidence in the structure itself, however, since the cooling rates depend very sensitively upon the difference between T_e and T_g , and this difference in the F-region approaches the combined experimental uncertainty of the temperature measurements. We believe, however, that the general increase of L_e with altitude reflects a real heat source.

The existence of such a source is even more clearly evident in satellite measurements of T_e at 1000 kilometers (Brace and Reddy, 1965) (Brace, et al., 1967) where the electron temperature over Wallops Island in this period is typically 1500 to 2000°K. These authors have suggested that these elevated temperature reflect a downward conduction of heat from the protonosphere at night. A gradient of 1°/km would be consistent with 6.11 measurements and would explain all of the heating above 200 kilometers. The fact that the Churchill nighttime L_e profile continues to decrease rapidly with altitude, and actually falls below the Wallops profile above 300 kilometers, is consistent with the absence of a protonosphere at this higher latitude. The negative temperature gradient above 260 kilometers (Figure 7) implies that heat is conducted upward into the upper F-region at night in the auroral zone.

E-region—The loss rates in the E-region evident in all of these flights, and in flights reported previously (Spencer, et al., 1965), are evidence for an E-region

source of electron heating. From these flights, as well as the earlier flights, a strong latitudinal dependence emerges; the highest loss rates occurring at Churchill. It is hoped that a recent day-night pair of launchings at Puerto Rico (latitude 18°N) will help extend the latitudinal coverage of this phenomenon. Initial analysis of these data suggests that much lower electron loss rates exist at this lower latitude. It is not yet clear whether Walker's mechanism of vibrationally excited N_2 (Walker, 1968) will be able to account for these E-region heating rates and for their geographical variation.

The possibility remains that the high E-region cooling rates reflect a systematic error in these and other probe measurements of T_e . However, it is difficult to explain how an instrumental error can produce the geographic dependence which the temperatures exhibit. It is even more puzzling since physically identical probes were employed at each location, and all were carried on ejected Thermosphere Probe payloads which did not differ significantly.

CONCLUSIONS

In summary, we conclude that the daytime middle latitude and auroral zone F-regions are both heated primarily by solar evf. This is confirmed by the good agreement between the electron cooling rate profiles and the electron heating rate profiles based exclusively on evf input. At night, the middle latitude F-region is heated primarily by heat conduction from the protonosphere, and the auroral zone ionosphere is heated by particle precipitation.

The E-region temperatures and electron loss rates give evidence for an electron heat source at both high and middle latitudes, both day and night, with significantly higher rates at higher latitudes.

ACKNOWLEDGMENTS

We thank J. A. Findlay for his aid in analyzing the data and Dr. J. G. Walker for valuable discussions concerning the interpretation of the data.

REFERENCES

- Banks, P. M., "Collision Frequencies and Energy Transfer of Ions" *Planet. Space Sci.*, 14, 1105-1122, 1965
- Brace, L. H., B. M. Reddy, "Early electrostatic probe results from Explorer 22," *J. Geophys. Res.*, 70, 5783-5792, 1965.
- Brace, L. H., N. W. Spencer, and G. R. Carignan, "Ionosphere electron temperature measurements and their implications," *J. Geophys. Res.*, 68, 5397-5412, 1963.
- Brace, L. H., N. W. Spencer, and A. Dalgarno, "Detailed behavior of the mid-latitude F-region from Explorer 17 satellite," *Planet. Space Sci.*, 13, 647-666, 1965.
- Brace, L. H., B. M. Reddy and H. G. Mayr, "Global behavior of the ionosphere at 1000 kilometer altitude," *J. Geophys. Res.*, 72, 265-283, 1967.
- Dalgarno, A. and T. C. Degges, "Electron cooling in the upper atmosphere," *Planet. Space Sci.*, 16, 125-127, 1968.
- Dalgarno, A., M. B. McElroy, and R. J. Moffett, "Electron temperature in the ionosphere," *Planet. Space Sci.*, 11, 463-484, 1963.
- Dalgarno, A., M. B. McElroy, and J. C. G. Walker, "The diurnal variation of ionospheric temperatures," *Planet. Space Sci.* 15, 331-345, 1967.
- Dalgarno A., J. C. G. Walker, "Ion temperatures in the topside ionosphere," *Planet. Space Sci.*, 15, 200-203, 1967.
- Dalgarno, A., M. B. McElroy, M. H. Rees, J. C. G. Walker, "The effects of

- oxygen cooling on ionospheric electron temperatures," (submitted to J.G.R.), 1968.
- Hanson, W. B., "Electron temperatures in the upper atmosphere," Space Res. III, 282-302, 1963.
- Jacchia, L. G., "The temperature above the thermopause," Smithsonian Astrophys. Observ. Report 150, April 22, 1964.
- Mott-Smith, H. M., I. Langmuir, "The theory of collectors in gaseous discharges," Phys. Rev., 28, 727, 1926.
- Nagy, A. F., J. C. G. Walker, "Direct measurements bearing on the question of the nighttime heating mechanism in the ionosphere," Planet. Space Sci, 15, 95-101, 1967.
- Rees, M. H., J. C. G. Walker, A. Dalgarno, "Auroral excitation of the forbidden lines of atomic oxygen," Planet. Space Sci, 15, 1097-1110, 1967.
- Spencer, N. W., L. H. Brace, G. R. Carignan, D. R. Taesch, and H. Nieman, "Electron and Molecular Nitrogen temperature and density in the thermosphere," J. Geophys. Res., 70, 2665-2698, 1965.
- Spencer, N. W., G. R. Carignan, D. R. Taesch, "Recent Measurements of the lower thermosphere structure," Meteorological Monograph of the American Meteorological Soc, 1967.
- Walker, J. C. G., "Electron and nitrogen vibrational temperature in the E-region of the ionosphere," Planet. Space Sci, 16, 1968.

Walker, J. C. G., L. H. Brace and M. H. Rees, "Langmuir probe evidence for a nocturnal ionization source at Fort Churchill, (submitted to J. Geophys. Res, 1968).

TABLE I

Flight	Date	GMT	LT	Location	F _{10.7}	Ap
NASA 6.11	20 Mar. 1965	05:42	00:42	Wallops*	74	7
18.01	19 Mar. 1965	18:09	13:09	Wallops	76	5
18.02	10 Nov. 1965	07:00	01:00	Churchill†	80	1
18.03	9 Nov. 1965	19:16	13:16	Churchill	80	4

LAT LONG

*Wallops Island 37°50' 75°29' W

†Churchill 58°44' 93°49' W

TABLE II

Tabulation of Measurements

Altitude (km)	WALLOPS ISLAND						FORT CHURCHILL						Altitude (km)		
	NASA 6.11 (Night)			NASA 18.01 (Day)			NASA 18.02 (Night)			NASA 18.03 (Day)					
	N _c		T _c (°K)	N _c		T _c	N _c		T _c	N _c		T _c			
	Up	Down	Up	Down	Up	Down	Up	Down	Up	Down	Up	Down			
100	3.0 (3)	4.0 (3)	1110	720	1.5 (5)	615	395	1.6 (4)	3.3 (4)	1150	520	1.8 (5)	830	895	100
110	-	5.0 (2)	-	785	1.6	700	450	2.5	4.7	1050	590	1.8	800	900	110
120	-	-	-	-	1.2	800	565	3.4	5.8	1000	660	1.7	830	925	120
130	6.0 (2)	5.8 (2)	1410	950	2.2	880	760	4.0	6.0	1000	735	1.6	905	955	130
140	8.5 (2)	8.0 (2)	1500	1050	2.7	990	895	4.3	6.2	1020	800	1.7	965	985	140
150	1.1 (3)	1.2 (3)	1580	1110	2.9	1070	1000	4.4	6.2	1050	880	1.9	1030	1020	150
160	1.2	1.5 (3)	1600	1200	3.2	1170	1090	4.5	6.5	1090	970	2.0	1090	1070	160
170	1.4	1.3 (3)	1580	1220	3.4	1270	1160	4.6	6.8	1130	1070	2.3	1170	1170	170
180	1.5	8.2 (2)	1440	1200	3.7	1310	1250	5.1	7.8	1160	1210	3.2	1250	1300	180
190	1.7	1.6 (3)	1300	1120	3.9	1410	1300	6.3	9.3	1200	1340	4.3	1360	1400	190
200	3.0	3.5 (3)	1140	1050	4.1	1470	1360	7.5	1.0 (5)	1230	1460	5.8	1470	1460	200
210	8.7	7.8 (3)	1050	985	4.3	1520	1420	8.8	1.1	1270	1580	6.1	1540	1500	210
220	2.1 (4)	2.3 (4)	1050	912	4.4	1570	1480	9.0	1.1	1370	1720	6.1	1550	1550	220
230	4.8	4.6 (4)	1100	850	4.5	1610	1520	9.1	1.0	1550	1880	6.0	1560	1600	230
240	9.0	7.5 (4)	1160	805	4.6	1650	1570	9.1	9.8 (4)	1760	1990	5.9	1570	1650	240
250	1.3 (5)	1.1 (5)	1110	780	4.7	1670	1610	9.0	9.3	1840	1990	5.7	1590	1700	250
260	1.7	1.5	1030	755	4.8	1700	1670	8.8	8.4	1780	1940	5.3	1630	1750	260
270	1.9	1.8	920	745	4.7	1720	1670	8.3	7.7	1800	1880	4.9	1670	1800	270
280	2.0	1.9	832	750	4.5	1750	1710	7.7	7.0	1640	1830	4.5	1720	1840	280
290	2.0	2.0	785	775	4.2	1770	1760	6.7	6.2	1570	1770	4.1	1780	1890	290
300	1.9	1.9	805	805	3.9	1800	1770	6.1	5.6	1500	1700	3.7	1840	1930	300
310	1.8	1.8	795	830	3.7	1810	1800	5.4	5.1	1430	1550	3.1	1900	1950	310
320	1.6	1.7	830	830	3.3	1820	1820	4.6	4.6	1270	1270	3.3	1960	1960	320
330	1.4	1.4	830	830	3.2	1820	1820	4.6	4.6	1270	1270	3.3	1960	1960	330

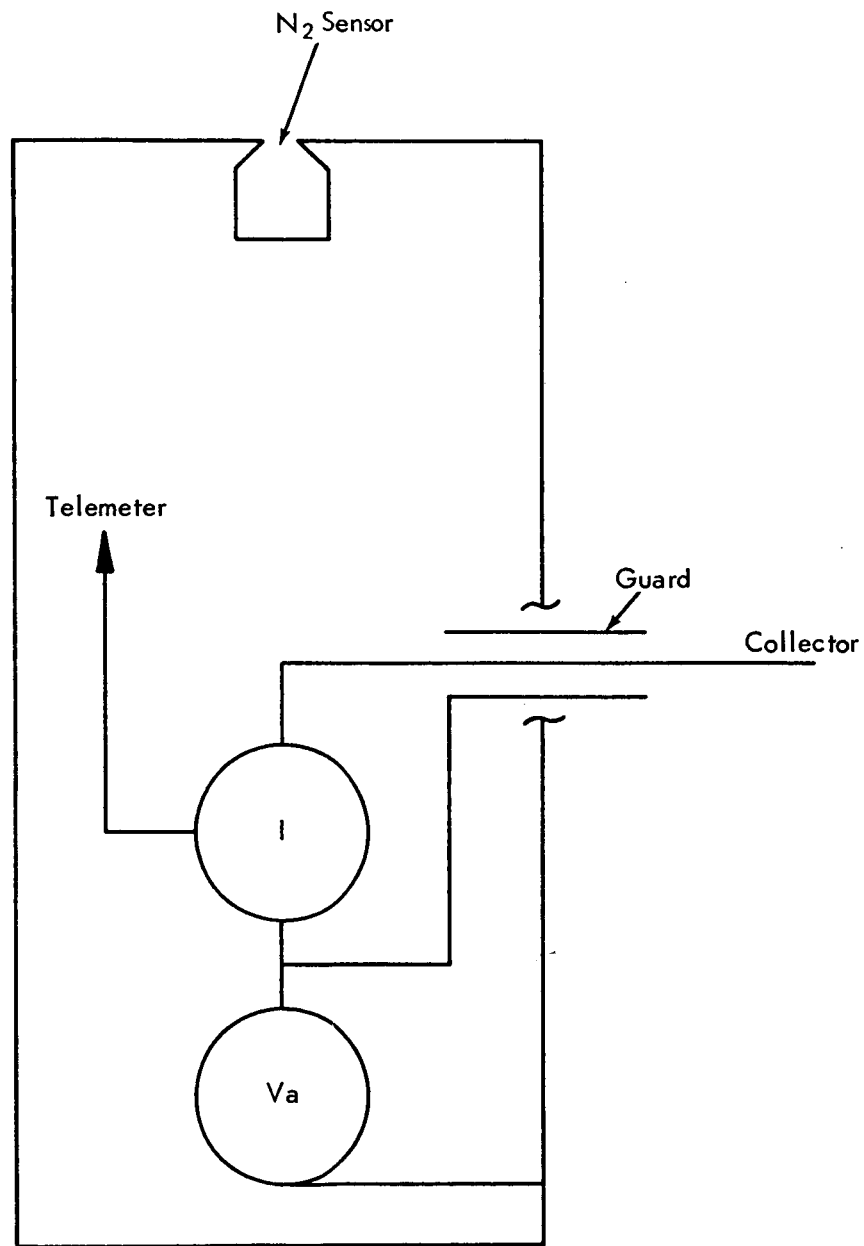


Figure 1. Electrical arrangement of the cylindrical probe experiment. The guard and collector are driven by same voltage sweep (-3v to +5v, -1v to +1.7v), and the collector current is telemetered. Three ranges of current sensitivity are employed (typically 0.1, 1.0, and 10 microamperes).

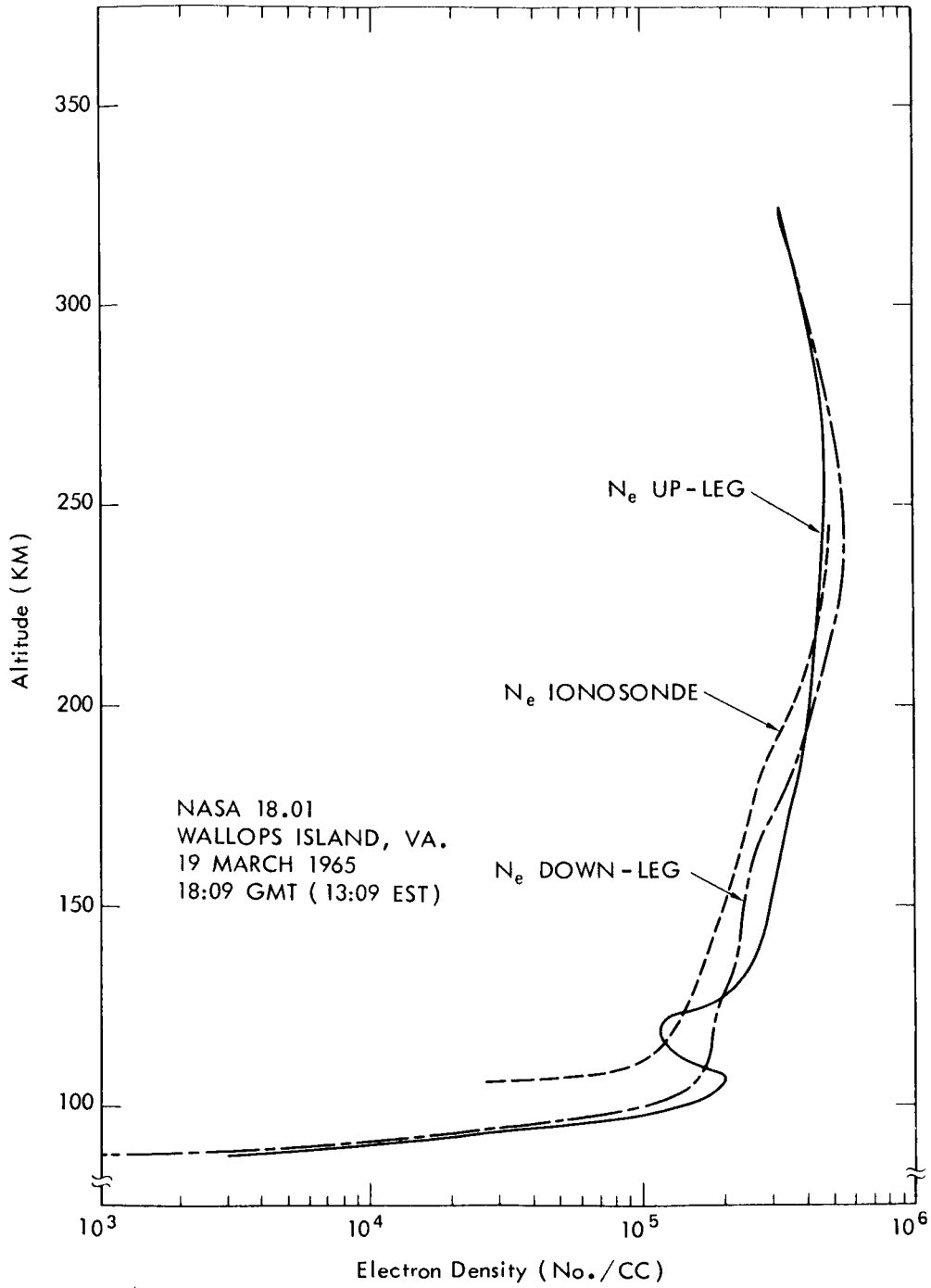


Figure 2. N_e profile from NASA 18.01, Wallops, Day.

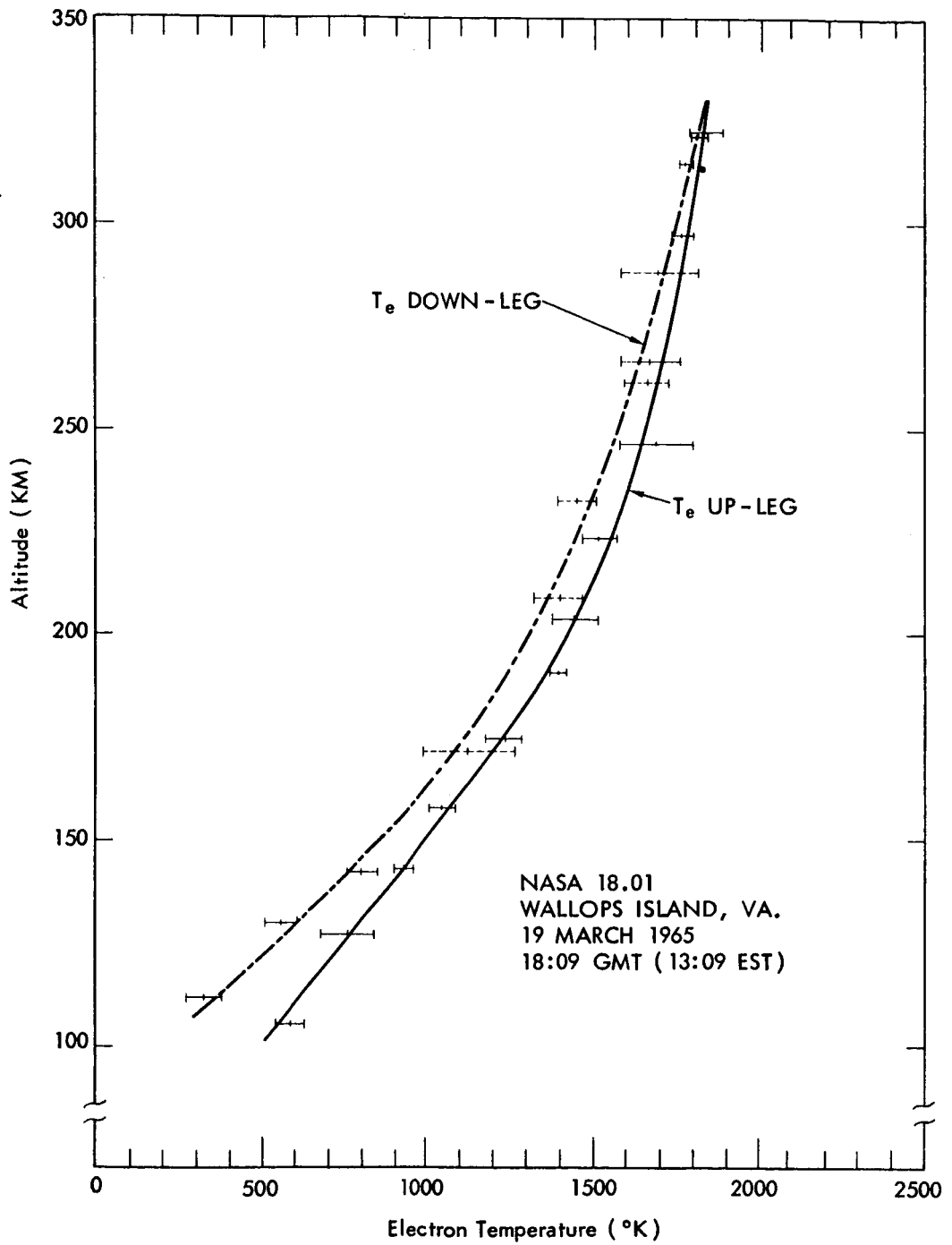


Figure 3. T_e profile from NASA 18.01, Wallops, Day.

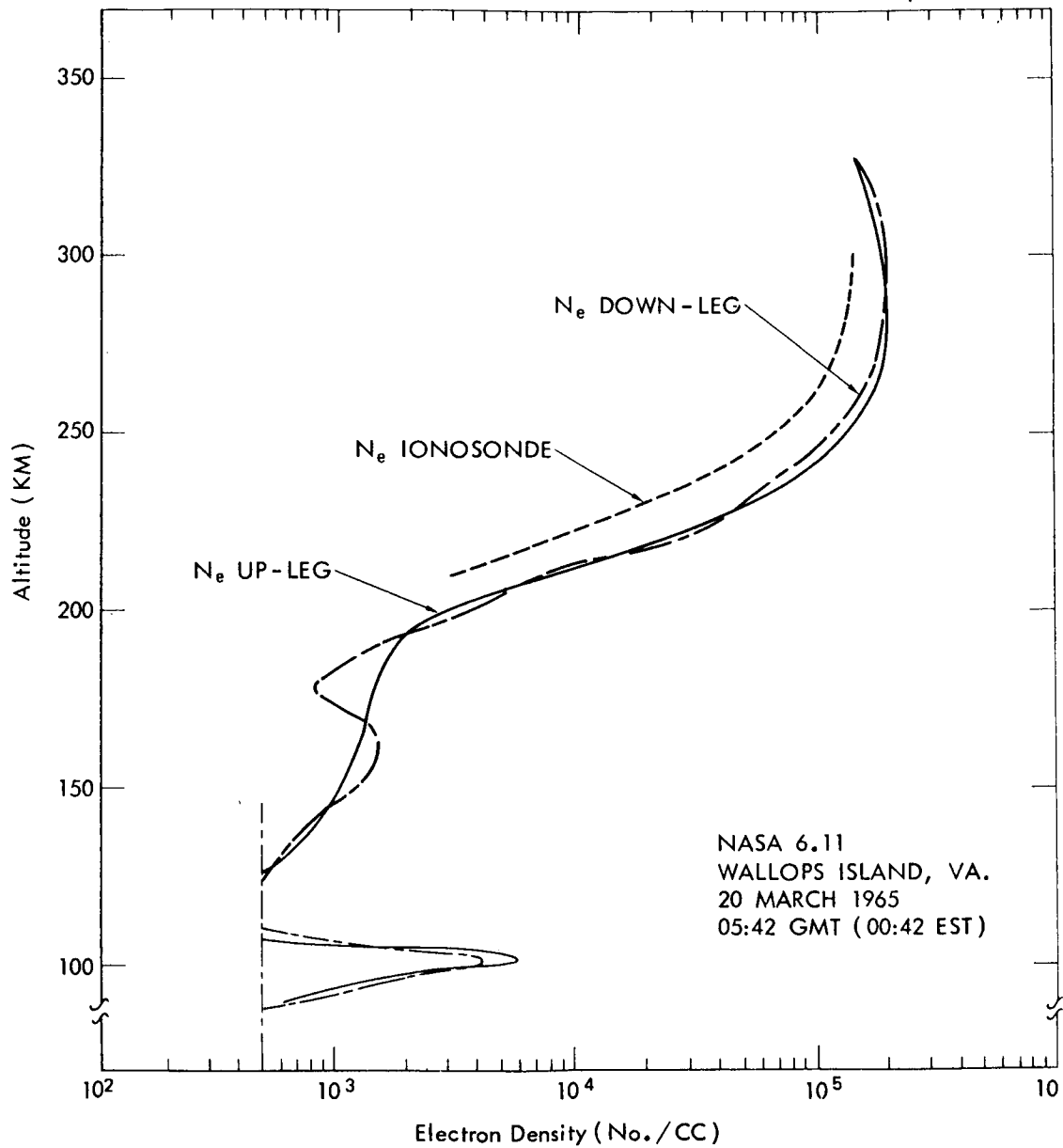


Figure 4. N_e profile from NASA 6.11, Wallops, Night. The vertical line at 5×10^2 /cc indicates the limit of resolution of N_e .

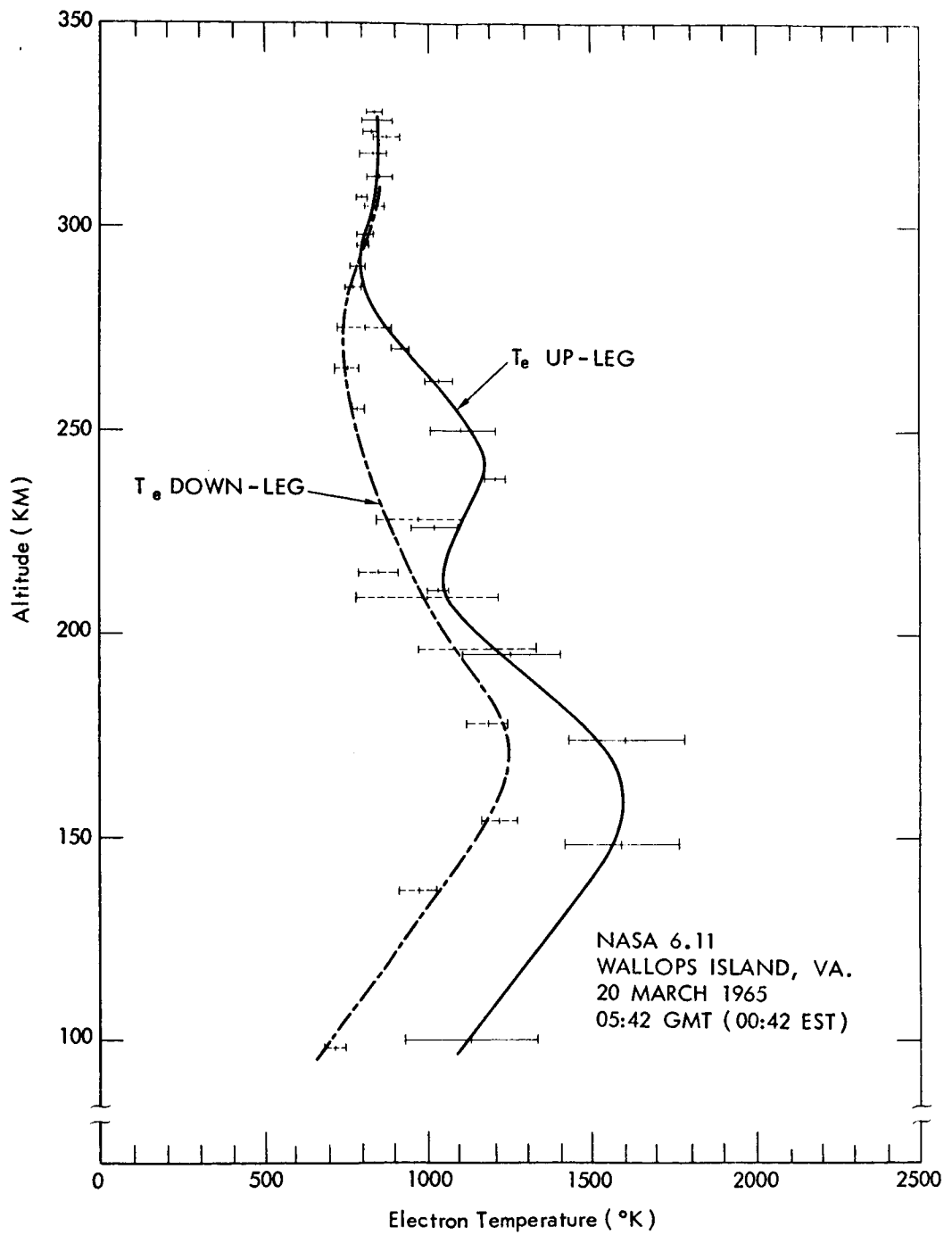


Figure 5. T_e profile from NASA 6.11, Wallops, Night.

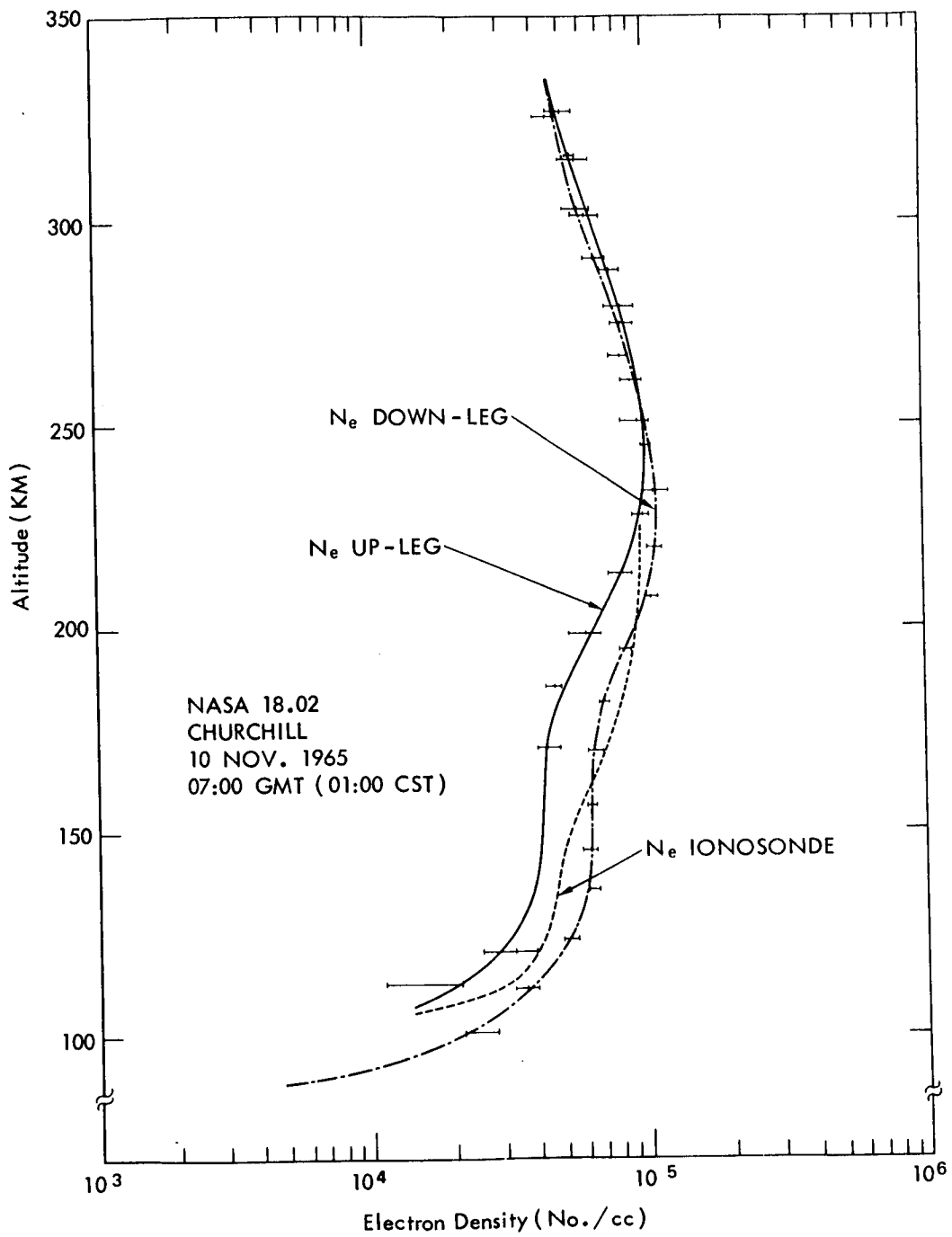


Figure 6. N_e profile from NASA 18.02, Churchill, Night.

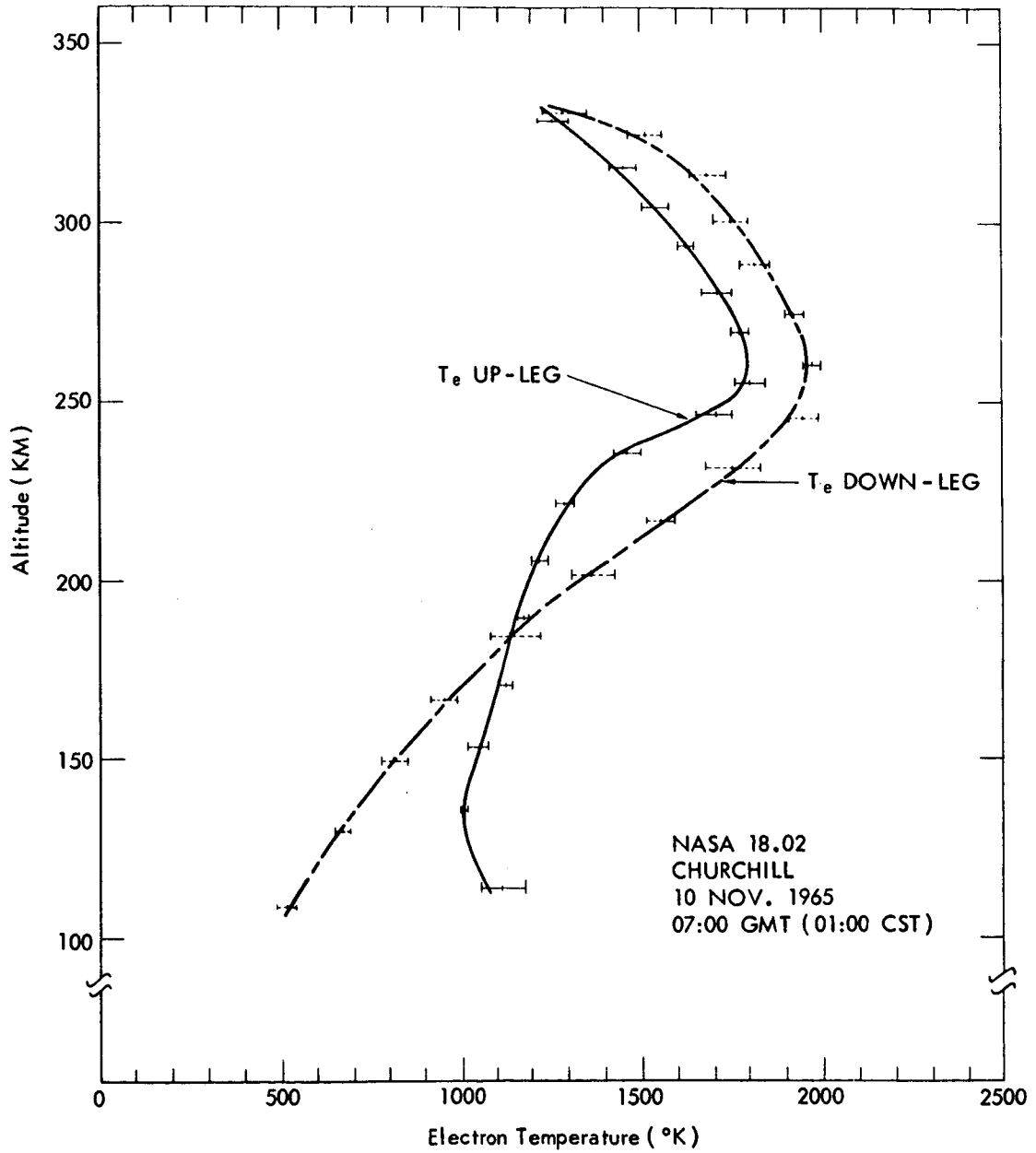


Figure 7. T_e profile from NASA 18.02, Churchill, Night.

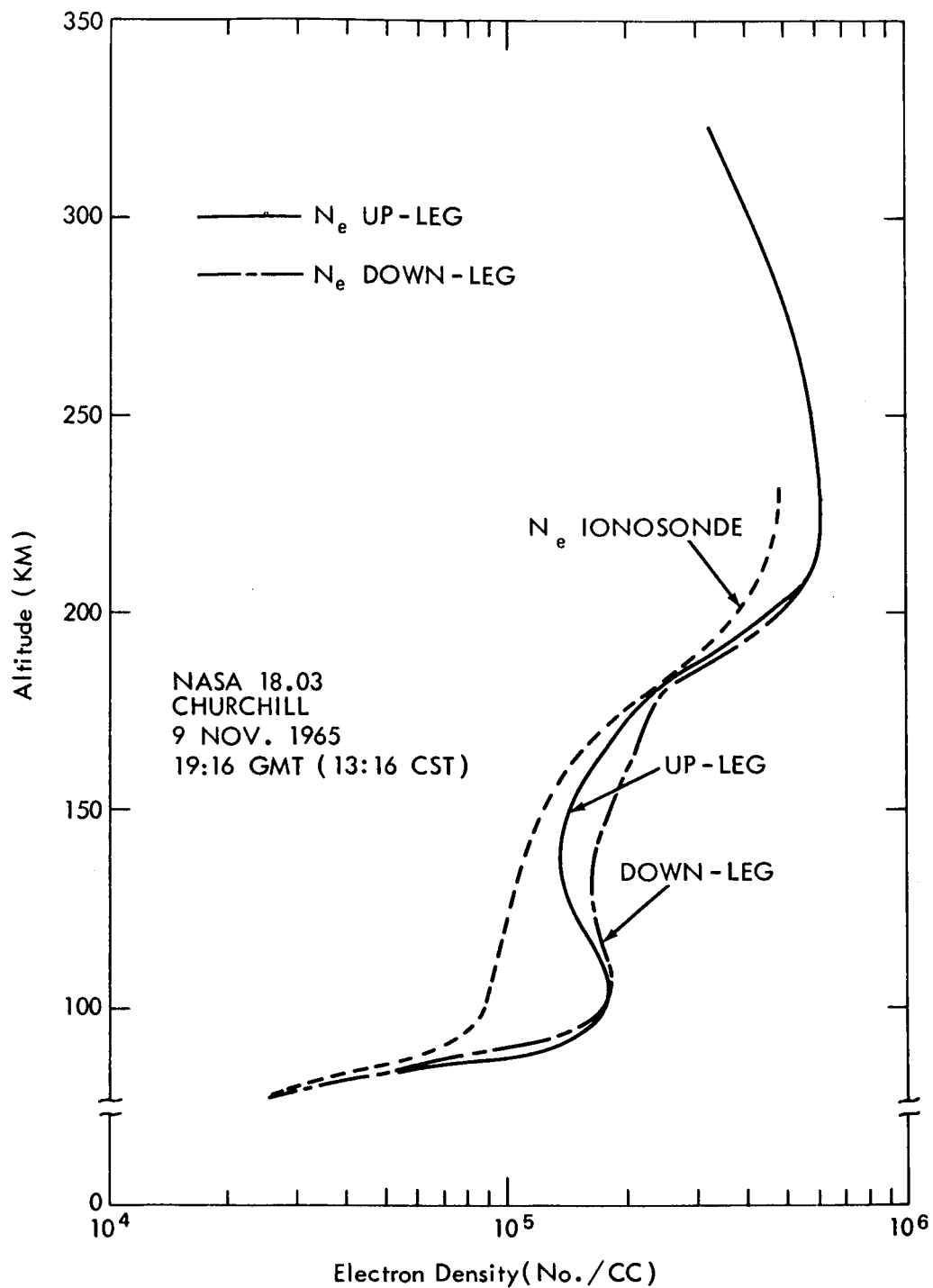


Figure 8. N_e profile from NASA 18.03, Churchill, Day.

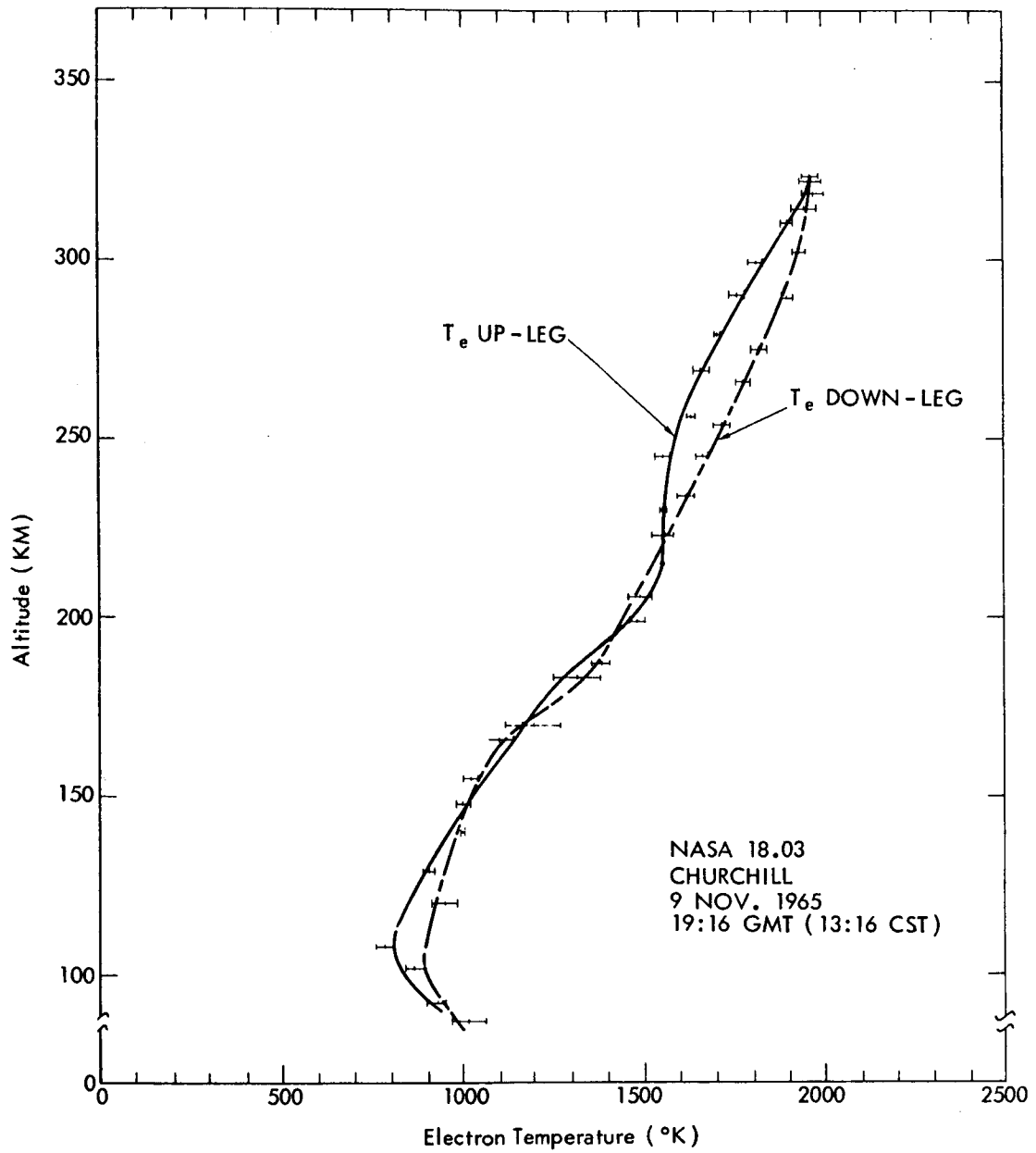


Figure 9. T_e profile from NASA 18.03, Churchill, Day.

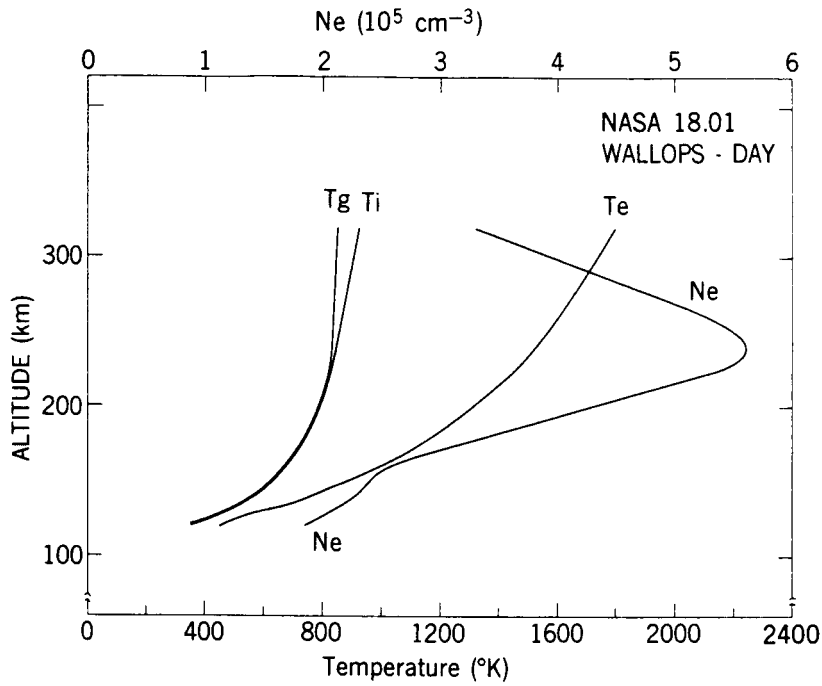


Figure 10. Composite profiles of NASA 18.01 showing measured T_e and N_e , calculated T_i and model T_g fitted to measured N_2 temperature.

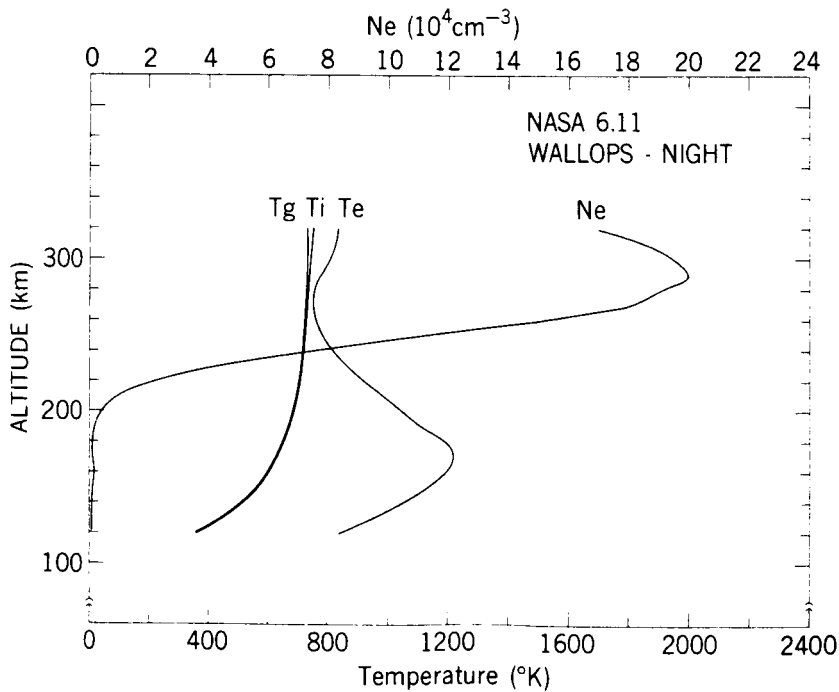


Figure 11. Composite profiles of NASA 6.11 showing measured T_e and N_e , calculated T_i and model T_g fitted to measured N_2 temperature.

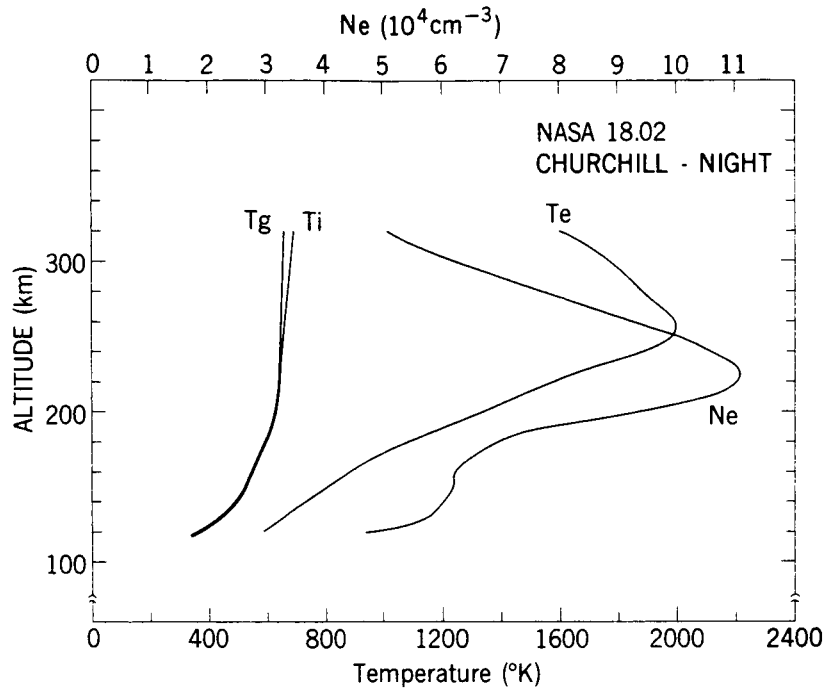


Figure 12. Composite profiles of NASA 18.02 showing measured T_e and N_e , calculated T_i and model T_g fitted to measured N_2 temperature.

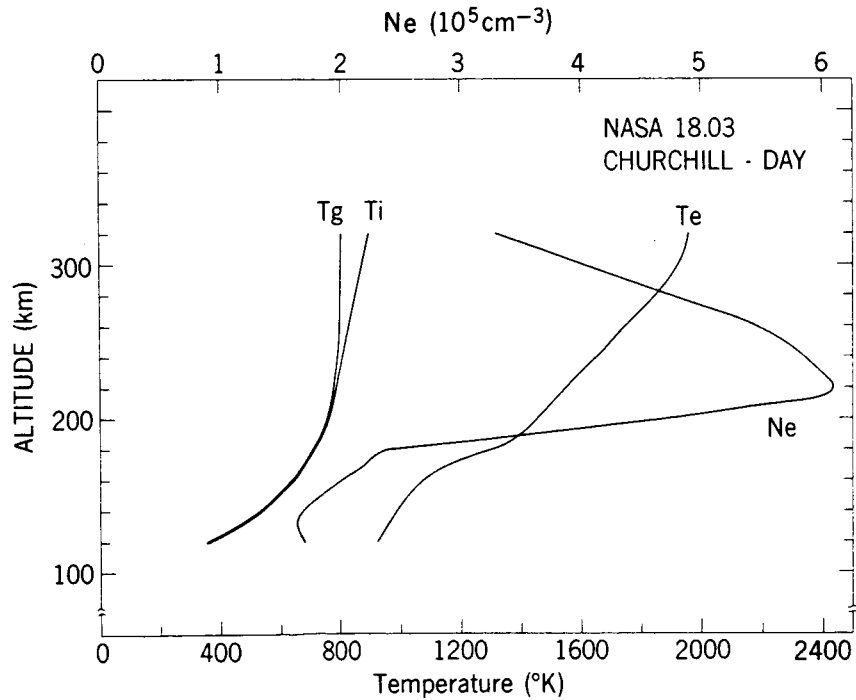


Figure 13. Composite profiles of NASA 18.03 showing measured T_e and N_e , calculated T_i and model T_g fitted to measured N_2 temperature.

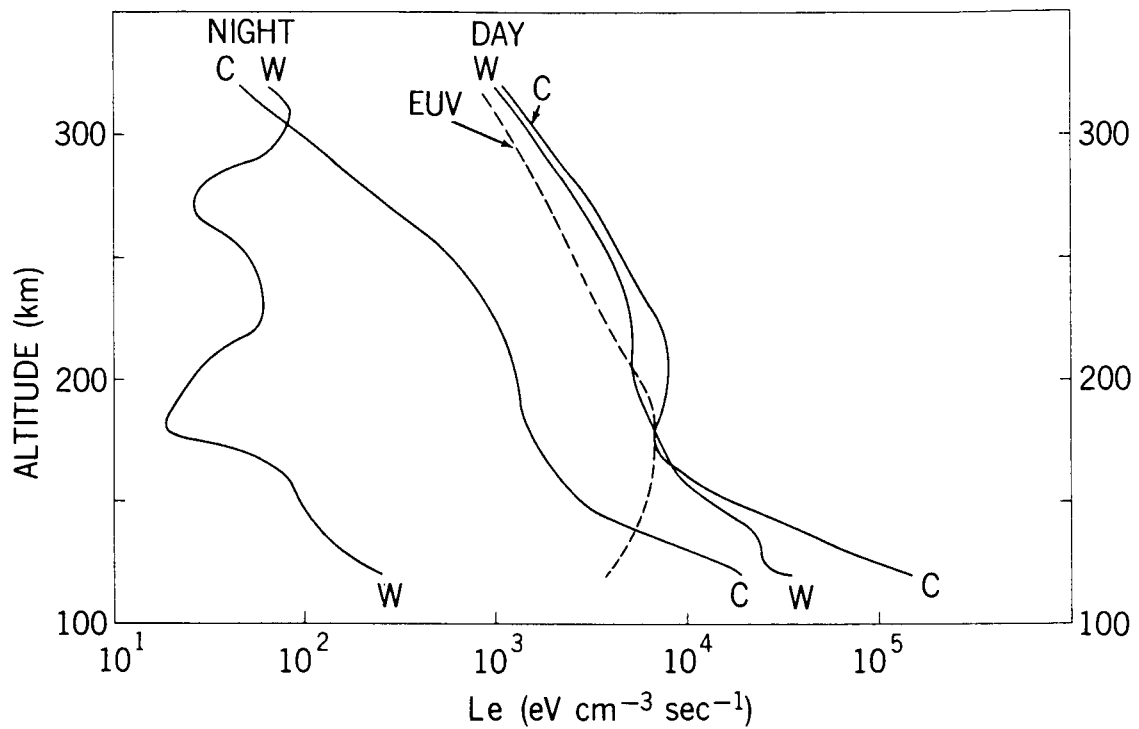


Figure 14. Electron loss rates, L_e , for NASA 18.01 (Day, W), NASA 6.11 (Night, W), NASA 18.02 (Night, C), NASA 18.03 (Day, C.). An evu heating rate calculated by Dalgarno, et al., (1967) is shown for comparison.